

# The anisotropic Kerr nonlinear refractive index of $\beta$ -BaB<sub>2</sub>O<sub>4</sub>

Morten Bache,<sup>1,\*</sup> Hairun Guo,<sup>1</sup> Binbin Zhou,<sup>1</sup> and Xianglong Zeng<sup>1,2</sup>

<sup>1</sup>*DTU Fotonik, Department of Photonics Engineering,*

*Technical University of Denmark, DK-2800 Kgs. Lyngby, Denmark*

<sup>2</sup>*The Key Lab of Specialty Fiber Optics and Optical Access Network, Shanghai University, 200072 Shanghai, China*

(Dated: March 14, 2019)

We study the anisotropic nature of the Kerr nonlinear response in a  $\beta$ -BaB<sub>2</sub>O<sub>4</sub> (BBO) crystal. The focus is on determining the relevant  $\chi^{(3)}$  cubic tensor components in connection with type I cascaded quadratic interaction, which is done by analyzing various experiments in the literature. We correct the data from some of the experiments for contributions from cascading as well as for updated material parameters, and find that the Kerr nonlinear refractive index used to model self-phase modulation in cascading is considerably larger than what has been used to date.

## I. INTRODUCTION

In cascaded second-harmonic generation (SHG) the phase mismatched nonlinear conversion process creates a strong Kerr-like nonlinear phase shift on the fundamental wave (FW) [1, 2]. This is in addition to the cubic (Kerr) nonlinearities that are always present in all media [3]. We can write the total refractive index of the pump

$$n = n_1 + \frac{1}{2}\Delta n_1 = n_1 + \frac{1}{2}|E_1|^2 n_{\text{cubic}} = n_1 + I_1 n_{\text{cubic}}^I \quad (1)$$

where  $n_1$  is the FW linear refractive index,  $E_1$  is the FW electric field, and  $I_1$  the FW intensity. It is typical to report the nonlinear refractive index relative to the electric field,  $n_{\text{cubic}}$ , or to the intensity,  $n_{\text{cubic}}^I$ . We have here for simplicity neglected cross-phase modulation (XPM) contributions since they are small in cascaded SHG. As mentioned we have contributions from both cascaded quadratic and cubic Kerr nonlinearities

$$n_{\text{cubic}}^I = n_{\text{casc}}^I + n_{\text{Kerr}}^I \quad (2)$$

where  $n_{\text{Kerr}}^I$  is the SPM Kerr nonlinear refractive index of the FW.

The contribution from the cascaded quadratic nonlinearities can in the strong cascading limit, where a large phase mismatch is assumed ( $\Delta k L \gg 1$ , where  $L$  is the length of the nonlinear crystal) and where pump depletion is neglected, be approximated as as [4]

$$n_{\text{casc}}^I = -\frac{4\pi d_{\text{eff}}^2}{c\varepsilon_0 \lambda_1 n_1^2 n_2 \Delta k} \quad (3)$$

where  $d_{\text{eff}}$  is the effective  $\chi^{(2)}$  nonlinearity. For  $\Delta k = k_2 - 2k_1 > 0$  the contribution is negative, i.e. self-defocusing. Here  $k_j = 2\pi/\lambda_j$  is the wavenumber.

The goal is to achieve a total self-defocusing nonlinearity  $n_{\text{cubic}}^I < 0$  by having a phase mismatch  $\Delta k > 0$ . When this happens, cascaded SHG becomes a simple and compact compressor system can compress femtosecond pulses

with multi-mJ pulse-energies because there are no self-focusing problems, and furthermore the pulses can be compressed with normal dispersion, which means anywhere in the visible and near-IR [5, 6]. A crucial requirement for this to happen is that  $|n_{\text{casc}}^I| > n_{\text{Kerr}}^I$ , and the soliton interaction depends critically on the  $n_{\text{Kerr}}^I$  value. Therefore, knowing an exact value of the  $n_{\text{Kerr}}^I$  coefficient is crucial.

A popular crystal for these cascading experiments is beta-barium-borate ( $\beta$ -BaB<sub>2</sub>O<sub>4</sub>, BBO), used in e.g. [5–11]. It has a decent quadratic nonlinear coefficient allowing for efficient type I ( $oo \rightarrow e$ ) SHG, it has low dispersion, a high damage threshold, and has believed to have a quite low Kerr nonlinearity. Here we formulate the interaction of the FW and SH waves, and we include the anisotropic nature of the frequency conversion crystal in the cubic nonlinearities. With this theoretical background, we then analyze several experiments, where the Kerr nonlinear refractive index was measured in BBO [11–17]. We show that the most important Kerr tensor component, which controls the FW SPM, is considerably higher than what has been reported and used until now. The analysis presented here should help understanding what exactly has been measured, and put the results into the context of cascaded quadratic soliton compression.

## II. THE ANISOTROPIC NONLINEAR TENSOR COMPONENTS

### A. Theory

In our previous work we studied type I interaction in a BBO crystal [10, 18–20]. There we assumed an isotropic Kerr nonlinear response, which implies

$$\chi_{\text{SPM}}^{(3)} = 3\chi_{\text{XPM}}^{(3)} \quad (4)$$

where  $\chi_{\text{SPM}}^{(3)}$  is the FW SPM coefficient, and  $\chi_{\text{XPM}}^{(3)}$  is the XPM coefficient. (Note that many previous publications erroneously have taken  $\chi_{\text{SPM}}^{(3)} = \chi_{\text{XPM}}^{(3)}$  in the type I configuration where the XPM terms are cross-polarized, and this mistake gives a 3 times too large XPM term. This

\* moba@fotonik.dtu.dk

identity  $\chi_{\text{SPM}}^{(3)} = \chi_{\text{XPM}}^{(3)}$  holds only in the type 0 configuration, where the XPM fields have identical polarizations.) In reality, all quadratic nonlinear crystals are anisotropic, and below we address this problem.

In cascaded soliton compression type I critical interaction in BBO is usually used, and few-cycle energetic pulses can be generated [5–7, 18–20], as well as soliton-induced Cherenkov radiation (dispersive waves) [10]. Here we study the anisotropic nature of the Kerr nonlinearity, and address the type I behaviour of BBO.

Let us write the basic propagation equations for degenerate SHG (i.e. either type 0, where the FW and SH fields are polarized along the same direction, or type I interaction, where the FW and SH are cross polarized). They describe in the slowly-varying envelope approximation the plane-wave interaction of the FW (frequency  $\omega_1$ , linear index  $n_1$ ) and the SH (frequency  $\omega_2 = 2\omega_1$ , linear index  $n_2$ ), and where cubic SPM and XPM effects are included. In mks units the equations for the electric fields are

$$\begin{aligned} & \left[ i\partial_z - \frac{1}{2}k_1^{(2)}(\omega_1)\partial_{\tau\tau} \right] E_1 + \frac{\omega_1 d_{\text{eff}}}{n_1 c} E_1^* E_2 e^{i\Delta k z} \\ & + \frac{3\omega_1}{8n_1 c} \left[ \chi_{\text{eff}}^{(3)}(\omega_1; \omega_1) E_1 |E_1|^2 + 2\chi_{\text{eff}}^{(3)}(\omega_1; \omega_2) E_1 |E_2|^2 \right] = 0 \end{aligned} \quad (5)$$

$$\begin{aligned} & \left( i\partial_z - id_{12}\partial_\tau - \frac{1}{2}k_2^{(2)}(\omega_2)\partial_{\tau\tau} \right) E_2 + \frac{\omega_1 d_{\text{eff}}}{n_2 c} E_1^2 e^{-i\Delta k z} \\ & + \frac{3\omega_2}{8n_2 c} \left[ \chi_{\text{eff}}^{(3)}(\omega_2; \omega_2) E_2 |E_2|^2 + 2\chi_{\text{eff}}^{(3)}(\omega_2; \omega_1) E_2 |E_1|^2 \right] = 0 \end{aligned} \quad (6)$$

The wave numbers are  $k_j(\omega) = n_j(\omega)\omega/c$ , the phase mismatch is  $\Delta k = k_2(\omega_2) - 2k_1(\omega_1)$ ,  $d_{12} = k_1^{(1)}(\omega_1) - k_2^{(1)}(\omega_2)$  is the group-velocity mismatch (GVM), and  $k_j^{(m)} \equiv d^m k_j / d\omega^m$  are the dispersion coefficients. For simplicity higher-order dispersion and self-steepening are neglected.

For an arbitrary input (i.e. FW) polarization various cascaded SHG processes can come into play ( $oo \rightarrow o$ ,  $oo \rightarrow e$ ,  $oe \rightarrow e$ ,  $oe \rightarrow o$ ,  $ee \rightarrow e$ , and  $ee \rightarrow o$ ). Their respective  $d_{\text{eff}}$ -values [16] for a crystal in the  $3m$  point group are

$$d_{\text{eff}}^{ooo} = -d_{22} \cos 3\phi \quad (7)$$

$$d_{\text{eff}}^{ooe} = d_{\text{eff}}^{oeo} = d_{31} \sin \theta - d_{22} \cos \theta \sin 3\phi \quad (8)$$

$$d_{\text{eff}}^{oee} = d_{\text{eff}}^{eoo} = d_{22} \cos^2 \theta \cos 3\phi \quad (9)$$

$$d_{\text{eff}}^{eee} = d_{22} \cos^3 \theta \sin 3\phi + 3d_{31} \sin \theta \cos^2 \theta + d_{33} \sin^3 \theta \quad (10)$$

The notation of the cubic nonlinearities is introduced as  $\chi_{\text{eff}}^{(3)}(\omega_i; \omega_j)$ , which implicitly assumes phase-matched SPM and XPM interaction between  $\omega_i$  and  $\omega_j$ , as opposed to general four-wave mixing. In presence of anisotropy, Eqs. (B13), (B14) and (B15) in [21] dictate for a type I interaction ( $oo \rightarrow e$ ) the cubic nonlinearities

are

$$\chi_{\text{eff}}^{(3)}(\omega_1; \omega_1) = c_{11} \quad (11)$$

$$\begin{aligned} \chi_{\text{eff}}^{(3)}(\omega_2; \omega_2) &= -4c_{10} \sin \theta \cos^3 \theta \sin 3\phi + c_{11} \cos^4 \theta \\ &+ \frac{3}{2}c_{16} \sin^2 2\theta + c_{33} \sin^4 \theta \end{aligned} \quad (12)$$

$$\chi_{\text{eff}}^{(3)}(\omega_1; \omega_2) = \frac{1}{3}c_{11} \cos^2 \theta + c_{16} \sin^2 \theta + c_{10} \sin 2\theta \sin 3\phi \quad (13)$$

Instead for a type 0  $ee \rightarrow e$  interaction, as recently considered for cascading quadratic nonlinearities in lithium niobate [22] and periodically poled lithium niobate [23, 24], we have

$$\chi_{\text{eff}}^{(3)}(\omega_1; \omega_1) = \chi_{\text{eff}}^{(3)}(\omega_2; \omega_2) = \chi_{\text{eff}}^{(3)}(\omega_1; \omega_2) \quad (14)$$

$$\begin{aligned} &= -4c_{10} \sin \theta \cos^3 \theta \sin 3\phi + c_{11} \cos^4 \theta \\ &+ \frac{3}{2}c_{16} \sin^2 2\theta + c_{33} \sin^4 \theta \end{aligned} \quad (15)$$

where  $c_{ij} \equiv \chi_{ij}^{(3)}$  and the shorthand notation  $ij$  is defined in App. B in [19]. In both cases  $\chi_{\text{eff}}^{(3)}(\omega_1; \omega_2) = \chi_{\text{eff}}^{(3)}(\omega_2; \omega_1)$ . The connections to the cubic nonlinear susceptibility are  $\chi_{\text{eff}}^{(3)}(\omega_i; \omega_j) = 4n_i n_{\text{Kerr}} / 3$  and  $\chi_{\text{eff}}^{(3)}(\omega_i; \omega_j) = 4n_i n_j \varepsilon_0 c n_{\text{Kerr}}^I / 3$ , cf. Eqs. (C4) and (C6) in [21]. Note that it is implicitly assumed that the chromatic dispersion of the nonlinearities is negligible. We will later use Miller's rule [25, 26] to scale the nonlinear coefficients to other wavelengths.

If the Kerr nonlinearity is considered isotropic, we have  $\chi_{\text{eff}}^{(3)}(\omega_1; \omega_2) = \chi_{\text{eff}}^{(3)}(\omega_1; \omega_1) / 3 = \chi_{\text{eff}}^{(3)}(\omega_2; \omega_2) / 3$  [type I  $oo \rightarrow e$  interaction, taking  $\theta = 0$  in Eqs. (11)-(13)], or  $\chi_{\text{eff}}^{(3)}(\omega_1; \omega_1) = \chi_{\text{eff}}^{(3)}(\omega_2; \omega_2) = \chi_{\text{eff}}^{(3)}(\omega_1; \omega_2)$  [type 0  $ee \rightarrow e$  interaction, cf. Eq. (14)].

For exploiting the cascaded nature of quadratic nonlinearities the by far most important component is the FW SPM coefficient  $\chi_{\text{eff}}^{(3)}(\omega_1; \omega_1)$ , and in a type I  $oo \rightarrow e$  configuration it is given by the  $c_{11}$  component. Instead in a type 0  $ee \rightarrow e$  interaction it is given by the expression from Eq. (15). The SH SPM and the XPM coefficients only play minor roles in extreme cases with very large intensities or large input fluence [19].

## B. Experimental background

Most experiments aiming to measure the Kerr nonlinear refractive index used Z-scan methods and often a nonlinear refractive index value was found without any mentioning of the tensorial nature of the cubic nonlinear susceptibility. The cascaded quadratic contributions were also often forgotten or assumed negligible.

There are also other issues with the Z-scan method that affect the measured nonlinear refractive index. If the repetition rate is too high, there will also be contributions to the measured  $n_{\text{Kerr}}^I$  from thermal effects as well as two-photon excited free carriers [27], and hence it does not contain just the instantaneous electronic, as

it is supposed to. For more on these issues, see e.g. [28]. Similarly, a long pulse duration can also lead to more contributions to the measured  $n_{\text{Kerr}}^I$  than just the electronic response that we aim to model, and in particular the static Raman contribution is measured as well. To see this consider the following form of a Kerr nonlinearity

$$\chi^{(3)}(t) = \chi_{\text{elec}}^{(3)}\delta(t) + \chi_R^{(3)}h_R(t) \quad (16)$$

where  $\chi_{\text{elec}}^{(3)}$  is the instantaneous electronic Kerr nonlinearity, and  $\chi_R^{(3)}h_R(t)$  is the delayed Kerr nonlinearity due to Raman phonon vibrations. It is custom to write

$$\chi^{(3)}(t) = \chi^{(3)}[(1 - f_R)\delta(t) + f_R h_R(t)] \quad (17)$$

where  $f_R$  is the fraction of Raman to the induced nonlinear polarization. The normalized Raman response function  $h_R(t)$  is usually modeled by a single (or a sum of) Lorentzian as

$$h_R(t) = \frac{\tau_1^2 + \tau_2^2}{\tau_1\tau_2} \exp(-t/\tau_2) \sin(t/\tau_1) H(t) \quad (18)$$

where  $\tau_1$  is the period of oscillations and  $\tau_2$  the decay time, and  $H(t)$  is the Heaviside step function ensuring causality. For a pulse much longer than the characteristic decay time the Z-scan method effectively measures the total Kerr nonlinearity  $\chi^{(3)} = \chi_{\text{elec}}^{(3)} + \chi_R^{(3)}$ .

### C. Measurements of $n_{\text{Kerr}}^I$ in the literature

We will now try to extract the values for BBO of each component in Eqs. (11)-(13). The value of the cubic nonlinear refractive index has been measured by several authors and for different pulse durations and crystal cuts. When converting from the nonlinear susceptibilities  $c_{ij} \equiv \chi_{ij}^{(3)}$  to the intensity nonlinear refractive index we use Eq. (C6) in [21]

$$n_{\text{Kerr},ij}^I = \chi_{ij}^{(3)} \frac{3}{4n_i n_j \epsilon_0 c} \quad (19)$$

Both are in mks (SI) units, and conversion to the esu system is also reported in [21].

DeSalvo et al. [13] used the Z-scan method with a 30 ps pulse at 1064 nm, which had  $\mathbf{k}$  parallel to the optical axis  $c$ , so  $\theta = 0$ . Thus, (a) the pump is always  $o$ -polarized no matter how the input beam is polarized, and (b) the input polarization determines the angle  $\phi$ . Since the specific orientation of the crystal with respect to the input polarization was not reported, we take it as unknown. The relevant Kerr contribution at the pump wavelength is  $oooo$  interaction, which is given by Eq. (11) as simply one tensor component  $c_{11}$ . The XPM contributions from interaction with the SH can safely be considered insignificant. The cascading contributions are from  $oo \rightarrow e$  and  $oo \rightarrow o$  processes. Since  $\theta = 0$  they have the

same phase mismatch values as  $e$ -polarized light in this case has the same refractive index as  $o$ -polarized light. At 1064 nm the value is  $\Delta k_{ooe} = \Delta k_{ooo} = 234 \text{ mm}^{-1}$ . Taking into account the two cascading channels Eqs. (8) and (7), and using Eq. (3), we get the total contribution  $n_{\text{casc}}^I = -[\sin^2(3\phi) + \cos^2(3\phi)]2.0 \cdot 10^{-20} \text{ m}^2/\text{W} = -2.0 \cdot 10^{-20} \text{ m}^2/\text{W}$ , i.e. independent on the propagation angle  $\phi$ . For these calculations we used  $d_{22} = -2.2 \text{ pm/V}$ . The  $d_{\text{eff}}$  values are typically reported with a 5% uncertainty [29], giving a 7% uncertainty on the cascading estimate. The experiment reported  $n_{\text{cubic}} = 11 \pm 2 \cdot 10^{-14} \text{ esu}$  at 1064 nm, and using Eq. (C11) in [21] this corresponds to  $n_{\text{cubic}}^I = 2.9 \pm 0.6 \cdot 10^{-20} \text{ m}^2/\text{W}$ . This means that when correcting for the cascading contributions we get

$$n_{\text{Kerr},11}^I = 4.9 \pm 0.6 \cdot 10^{-20} \text{ m}^2/\text{W}, \lambda = 1.064 \mu\text{m} \quad (20)$$

We can proceed with their measurement at 532 nm, where  $n_{\text{cubic}} = 21 \pm 4 \cdot 10^{-14} \text{ esu}$  was measured, corresponding to  $n_{\text{cubic}}^I = 5.3 \pm 1.0 \cdot 10^{-20} \text{ m}^2/\text{W}$ . The cascading is smaller here, using  $\Delta k_{ooe} = \Delta k_{ooo} = 1,933 \text{ mm}^{-1}$  we get  $n_{\text{casc}}^I = -0.61 \cdot 10^{-20} \text{ m}^2/\text{W}$  (where we used  $d_{22} = 2.6 \text{ pm/V}$  as measured at 532 nm [29]), so

$$n_{\text{Kerr},11}^I = 5.9 \pm 1.0 \cdot 10^{-20} \text{ m}^2/\text{W}, \lambda = 0.532 \mu\text{m} \quad (21)$$

At 355 nm  $n_{\text{cubic}} = 14 \pm 3 \cdot 10^{-14} \text{ esu}$  was measured, corresponding to  $n_{\text{cubic}}^I = 3.4 \pm 0.7 \cdot 10^{-20} \text{ m}^2/\text{W}$ . The cascading is small, using  $\Delta k_{ooe} = \Delta k_{ooo} = 11,736 \text{ mm}^{-1}$  we get  $n_{\text{casc}}^I = -0.18 \cdot 10^{-20} \text{ m}^2/\text{W}$  (where the  $d_{22}$  coefficient was appropriately converted to 355 nm using Miller's scaling), so

$$n_{\text{Kerr},11}^I = 3.6 \pm 0.7 \cdot 10^{-20} \text{ m}^2/\text{W}, \lambda = 0.355 \mu\text{m} \quad (22)$$

Finally, at 266 nm they measured  $n_{\text{cubic}} = 1 \pm 0.3 \cdot 10^{-14} \text{ esu}$ . At this wavelength cascading is estimated to be insignificant (certainly we cannot estimate accurately it using the Sellmeier equations as the SH lies beyond the UV pole), so  $n_{\text{cubic}} \simeq n_{\text{Kerr}}$ , and converting to SI we have

$$n_{\text{Kerr},11}^I = 0.24 \pm 0.07 \cdot 10^{-20} \text{ m}^2/\text{W}, \lambda = 0.266 \mu\text{m} \quad (23)$$

In a similar experiment, Li et al. [15] pumped a 5 mm z-cut BBO crystal with 150 fs 780 nm pulses from a Ti:sapphire oscillator. The propagation was also here along the optical axis, implying  $\theta = 0$  and thus that for both cascading and Kerr nonlinearities the angle  $\phi$  should not matter. Nonetheless, they measured using the Z-scan method two different results when flipping the input polarization, namely  $n_{\text{cubic}}^I = 4.0 \pm 0.5 \cdot 10^{-20} \text{ m}^2/\text{W}$  when polarizing light along the  $[1 \ 0 \ 0]$  direction ( $x$ -axis, i.e.  $\phi = 0$ ), and  $n_{\text{cubic}}^I = 3.2 \pm 0.5 \cdot 10^{-20} \text{ m}^2/\text{W}$  when polarizing light along the  $[0 \ 1 \ 0]$  direction ( $y$ -axis, i.e.  $\phi = \pi/2$ ). Cascading was neglected, so let us assess whether this is true. As above, the cascading contributions are from  $oo \rightarrow e$  and  $oo \rightarrow o$ , both having the same

$\Delta k_{ooe} = \Delta k_{ooo} = 552 \text{ mm}^{-1}$ , and the total cascading becomes  $n_{\text{casc}}^I = -1.2 \cdot 10^{-20} \text{ m}^2/\text{W}$ . This must be considered a significant contribution. Thus, when correcting the measured nonlinearities we get

$$n_{\text{Kerr},11}^I = 5.2 \pm 0.5 \cdot 10^{-20} \text{ m}^2/\text{W}, \quad (24)$$

$$[1 \ 0 \ 0], \lambda = 0.78 \ \mu\text{m}$$

$$n_{\text{Kerr},11}^I = 4.4 \pm 0.5 \cdot 10^{-20} \text{ m}^2/\text{W}, \quad (25)$$

$$[0 \ 1 \ 0], \lambda = 0.78 \ \mu\text{m}$$

The repetition rate was 76 MHz, but they saw the same results using a 760 kHz repetition rate.

Ganeev et al. [17] used the Z-scan method, and the pump was a 2 Hz 55 ps 1064 nm pulse. The crystal was pumped at  $\theta = 51^\circ$ . This choice was motivated by making cascading negligible. The procedure they used was to calculate the "critical"  $\Delta k_c$  where defocusing cascading exactly balances the intrinsic focusing Kerr, i.e. where  $|n_{\text{casc}}^I| = n_{\text{Kerr}}^I$ . By angle tuning well away from this point (so  $\Delta k \gg \Delta k_c$ ) they tried to make cascading insignificant. We estimate this to be true: specifically, we assume the pump is *o*-polarized, and that  $\phi = \pi/6$  to optimize SHG. Then the only cascading channel is  $oo \rightarrow e$ , with  $\Delta k_{ooe} = -655 \text{ mm}^{-1}$ , and  $n_{\text{casc}}^I = 0.31 \cdot 10^{-20} \text{ m}^2/\text{W}$  is therefore self-focusing (as they also note themselves). They measured  $n_{\text{Kerr},11}^I = 7.4 \pm 2.2 \cdot 10^{-20} \text{ m}^2/\text{W}$  with the uncertainty estimated to be 30%, so correcting for cascading

$$n_{\text{Kerr},11}^I = 7.1 \pm 2.2 \cdot 10^{-20} \text{ m}^2/\text{W}, \lambda = 1.064 \ \mu\text{m} \quad (26)$$

Repeating the same procedure at 532 nm they measured  $n_{\text{Kerr},11}^I = 8.0 \pm 2.4 \cdot 10^{-20} \text{ m}^2/\text{W}$ . However, now cascading is more significant as  $\Delta k_{ooe} = -194 \text{ mm}^{-1}$ , and  $n_{\text{casc}}^I = 2.8 \cdot 10^{-20} \text{ m}^2/\text{W}$ . Therefore the Kerr value corrected for cascading becomes

$$n_{\text{Kerr},11}^I = 5.2 \pm 2.4 \cdot 10^{-20} \text{ m}^2/\text{W}, \lambda = 0.532 \ \mu\text{m} \quad (27)$$

Hache et al. [12] performed a Z-scan measurement on a 1 mm BBO cut at  $\theta_c = 29.2^\circ$  with 800 nm 100 fs pulses from a Ti:sapphire amplifier. The pump was *o*-polarized allowing for  $oo \rightarrow e$  cascading interaction. They measured the total nonlinear phase shift close to the phase-matching point  $\theta_c$  and "far from SHG phase matching" they found a nonlinear phase shift, which they claim is equivalent to the Kerr nonlinear index (i.e. no cascading contributions)

$$n_{\text{Kerr},11}^I = 4.5 \pm 1.0 \cdot 10^{-20} \text{ m}^2/\text{W}, \lambda = 0.8 \ \mu\text{m} \quad (28)$$

Whether any cascading contributions did contribute nonetheless cannot be judged with the information at hand, as they did not specify the angle they used for this measurement.

Moses et al. [11] pumped a BBO crystal at 800 nm with 110 fs *o*-polarized light and angle-tuning the crystal to get zero nonlinear refraction: this happens when the

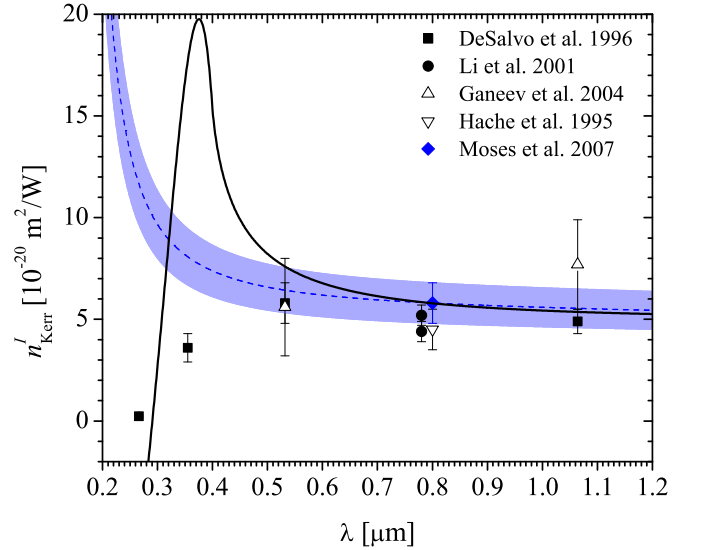


FIG. 1. Summary of the experimental data for  $n_{\text{Kerr},11}^I$  presented in Eqs. (20)-(29). Thick curve: Predicted  $n_{\text{Kerr},el}^I$  [31] using  $K = 3100 \text{ eV}^{3/2} \text{ cm}/\text{GW}$  and  $E_g = 6.2 \text{ eV}$  [13]. Dashed blue curve: the data from Eq. (29) extended to other wavelengths using Miller's scaling. The shaded area indicates the uncertainty.

cascading from the  $oo \rightarrow e$  interaction exactly balances the Kerr nonlinear refraction, which was found to occur at  $\Delta k = 31 \pm 5 \text{ } \pi/\text{mm}$  for a wide range of intensities. Using this phase mismatch value and that  $n_{\text{cubic}}^I = 0$  then a reverse calculation gives  $n_{\text{Kerr}}^I = -n_{\text{casc}}^I$ . Using the value  $d_{\text{eff}} = 1.8 \text{ pm}/\text{V}$  they inferred the value  $n_{\text{Kerr}}^I = 4.6 \pm 0.9 \cdot 10^{-20} \text{ m}^2/\text{W}$  (the main source of the uncertainty lies in determining the precise phase-mismatch value). Since *o*-polarized pump light was used, this contains only the  $c_{11}$  tensor contribution from an  $oooo$  interaction. However, the value  $d_{\text{eff}} = 1.8 \text{ pm}/\text{V}$  they used to infer this nonlinearity was probably taken too low [30]. Let us therefore estimate it again using a more accurate value:  $\Delta k = 31 \text{ } \pi/\text{mm}$  is achieved at 800 nm with  $\theta = 26.0^\circ$ , giving  $d_{\text{eff}} = 2.09 \text{ pm}/\text{V}$  using  $d_{22} = -2.3 \text{ pm}/\text{V}$  and  $d_{31} = 0.04 \text{ pm}/\text{V}$ . With this corrected value we get

$$n_{\text{Kerr},11}^I = 5.8 \pm 1.0 \cdot 10^{-20} \text{ m}^2/\text{W}, \lambda = 0.8 \ \mu\text{m} \quad (29)$$

This completes the  $c_{11}$  measurements. A summary of the data is shown in Fig. 1, together with the predicted electronic nonlinearity from the 2-band model. The data are not too far away from this theoretical curve, but on the other hand the predicted strong enhancement just below 400 nm cannot be confirmed experimentally. This is of little importance for our purpose, however, because in cascaded SHG the FW wavelength is usually never below 600 nm. We also show the value of Moses et al., Eq. (29), and how using Miller's scaling it translates to other wavelengths. We see that this measurement is a quite good representative of the other data points in the visible (except below 500 nm) and the near-IR.

Banks et al. [16] measured the  $c_{10}$  tensor component of BBO using THG measurements at 1053 nm using 350 fs pulses, and if using the quadratic nonlinear coefficients of Shoji et al. [29] they got  $C_{10} = -6 \cdot 10^{-24} \text{ m}^2/\text{V}^2$ . (They extracted other values as well, but we choose to use this one because it was calculated from the experimental data using the same effective quadratic nonlinearities of Shoji et al. as we use. In fact, Banks et al. reported the  $c_{10}$  value came with a quite large uncertainty due to the uncertainty in the  $d_{31}$  – and  $d_{15}$ , in absence of Kleinman symmetry – coefficients in the literature.) Since [16] define  $C_{ij} = \chi_{\text{eff},ij}^{(3)}/4$  this gives in our notation  $c_{10} = -24 \cdot 10^{-24} \text{ m}^2/\text{V}^2$  corresponding to

$$n_{\text{Kerr},10}^I = -0.25 \pm 0.04 \cdot 10^{-20} \text{ m}^2/\text{W}, \lambda = 1.053 \mu\text{m} \quad (30)$$

The uncertainty of the measurement was not reported, but for a similar fit it was reported to be 15%, which is what we used above.

Banks et al. [16] also measured the mixture  $\frac{1}{3}C_{11} \cos^2 \theta_m + C_{16} \sin^2 \theta_m = 4.0 \pm 0.2 \cdot 10^{-23} \text{ m}^2/\text{V}^2$  at  $\theta_m = 47.7^\circ$ . If we now use  $n_{\text{Kerr},11}^I = 4.9 \cdot 10^{-20} \text{ m}^2/\text{W}$  from DeSalvo et al. we can calculate the  $c_{16}$  component as  $n_{\text{Kerr},16}^I = 1.7 \pm 0.3 \cdot 10^{-20} \text{ m}^2/\text{W}$ . If we instead use the Moses et al. result (appropriately scaled to 1053 nm using Miller's scaling) then we get

$$n_{\text{Kerr},16}^I = 1.5 \pm 0.4 \cdot 10^{-20} \text{ m}^2/\text{W}, \lambda = 1.053 \mu\text{m} \quad (31)$$

Sheik-Bahae and Ebrahimzadeh [14] used the Z-scan method to measure  $n_{\text{cubic}}^I = 3.65 \pm 0.6 \cdot 10^{-20} \text{ m}^2/\text{W}$  using a 120 fs pump pulse at  $\lambda = 0.850 \mu\text{m}$ . The BBO crystal was cut for phase matching at 800 nm, i.e. with  $\theta = 29.2^\circ$ . The pump pulse was  $e$ -polarized as to ensure lack of phase matching and thereby no cascading. We will now assess whether this assumption is fulfilled. First, let us mention that using  $e$ -polarized light means that several tensor components come into play: the effective Kerr nonlinearity at the pump wavelength is an  $eeee$  interaction (again we can safely neglect the XPM contributions), which is given by Eq. (15). For  $\theta = 29.2^\circ$  the effective nonlinearity is

$$\chi_{\text{eff}}^{(3)} = -1.3c_{10} \sin 3\phi + 0.58c_{11} + 0.36c_{16} + 0.06c_{33} \quad (32)$$

Four tensor components appear, although the low prefactor to the  $c_{33}$  component makes its contribution negligible. We point out that the  $c_{10}$  component can be removed by taking  $\phi = 0$ , and it can be maximized by taking  $\phi = \pi/6$ . This being a crystal cut for optimal SHG at 800 nm, it would be a safe assumption to take  $\phi = \pi/6$  as this optimizes the  $d_{\text{eff}}$  nonlinearity, see Eq. (8).

The cascading contributions are  $ee \rightarrow o$  and  $ee \rightarrow e$ . The phase mismatch values for  $\theta = 29.2^\circ$  are  $\Delta k_{eeo} = 870 \text{ mm}^{-1}$  and  $\Delta k_{eee} = 396 \text{ mm}^{-1}$ . The cascading contributions depend strongly in  $\phi$ , but at  $\phi = \pi/6$  the sum is  $n_{\text{casc}}^I = -0.7 \cdot 10^{-20} \text{ m}^2/\text{W}$ . For these calculations we used

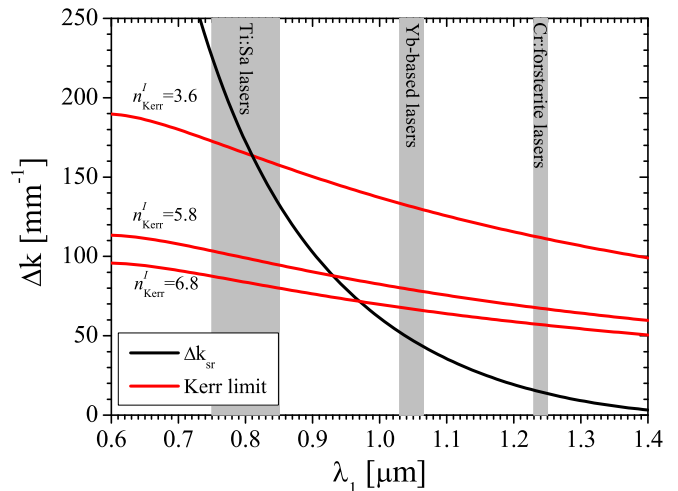


FIG. 2. Compression diagram for BBO type I cascaded SHG. For various pump wavelengths  $\lambda_1$  the choice of phase-mismatch parameter  $\Delta k$  affects the compression. In order to excite solitons the phase-mismatch must be kept below the Kerr limit (red line), because otherwise the cubic nonlinearities are too strong ( $n_{\text{Kerr},11}^I > n_{\text{casc}}^I$ ). Optimal compression occurs when the cascaded nonlinearities dominate over GVM effects ( $\Delta k > \Delta k_{\text{sr}}$ , above the black line). Note that for  $\lambda_1 > 1.49 \mu\text{m}$  the FW GVD becomes anomalous. Thus, the self-defocusing nonlinearity can no longer be balanced, and self-defocusing solitons are no longer supported. We have also indicated the operation wavelengths of Cr:forsterite, Yb and Ti:Sapphire based amplifiers. The red lines use Miller's rule to estimate the nonlinear quadratic and cubic susceptibilities at other wavelengths.

$d_{22} = -2.3 \text{ pm}/\text{V}$  as measured at 852 nm. With these values we can conclude that by choosing  $e$ -polarized light the cascading contributions are minimized, but they are not insignificant (they are roughly equal to the reported uncertainty of  $\pm 0.6 \cdot 10^{-20} \text{ m}^2/\text{W}$ .) If we now correct the measured value with the cascading contributions (using the value  $n_{\text{casc}}^I = -0.7 \cdot 10^{-20} \text{ m}^2/\text{W}$ ) at  $\phi = \pi/6$  we get  $n_{\text{Kerr}}^I = 4.3 \cdot 10^{-20} \text{ m}^2/\text{W}$ . We remind that this value is a mixture of difference tensor components, cf. Eq. (32).

Let us try to evaluate whether this measurement agrees with any of the previous one: Using Eq. (30) from Banks et al. and Eq. (29) from Moses et al., then from Eq. (32) we can calculate  $n_{\text{Kerr},16}^I = 1.7 \cdot 10^{-20} \text{ m}^2/\text{W}$ . This is not too far off the value found in Eq. (31). In a similar way we used the other  $n_{\text{Kerr},11}^I$  values (except the two measurements below 400 nm by DeSalvo et al.), and the  $n_{\text{Kerr},16}^I$  values we extract lie in the range between 1.1-2.0. Therefore we stick to the value reported in Eq. (31).

#### D. Implications for cascaded pulse compression in BBO

In some of our previous work related to BBO [18–20], we assumed an isotropic Kerr nonlinearity, and have used

the value  $n_{\text{Kerr}}^I = 3.65 \cdot 10^{-20} \text{ m}^2/\text{W}$  taken from [14], and in a later publication, we have used a value similar to Eq. (29). An implication of this larger value is that the "compression window" [19] becomes smaller. With this we imply a range of phase-mismatch values, where compression is optimal. We first need  $\Delta k$  to be small enough so  $n_{\text{cubic}}^I < 0$ , i.e.  $|n_{\text{casc}}^I| > n_{\text{Kerr},11}^I$ . This is the upper end of the window, also denoted the Kerr limit. The smaller  $\Delta k$  we now take the stronger the cascading nonlinearity. However, at a certain point the GVM becomes too strong and the compression quality is strongly reduced. Several things happen: (a) the GVM-induced self-steepening term [7] is increased as it scales as  $d_{12}/\Delta k$ , so the compressed pulse experiences a strong pulse-front shock. (b) Below a certain limit, denoted the stationary threshold [18], the SH will experience a resonant phase matching condition of a sideband frequency to the pump spectrum. This is damaging to pulse compression because in the cascading process effectively this is the cascading bandwidth felt by the FW, and in the transition from the stationary to the nonstationary regime, the bandwidth essentially goes from being octave spanning to becoming resonant and thereby narrow [22]. The criterion for being in the stationary regime is, in the simple case where only second-order dispersion is considered [18], that  $d_{12}^2 - 2k_2^{(2)}\Delta k < 0$ , so in the case where the SH GVD is normal (positive) we have the stationary regime with broadband cascading when

$$\Delta k > \Delta k_{\text{sr}} \equiv \frac{d_{12}^2}{2k_2^{(2)}(\omega_2)} \quad (33)$$

While decent compression may occur also below this threshold, the pulse quality is not nearly as good and can only be done with very low effective soliton orders [21]. The implications of the larger nonlinear SPM Kerr nonlinearity for the FW is visualized in Fig. 2. With the lower value,  $n_{\text{Kerr}}^I = 3.65 \cdot 10^{-20} \text{ m}^2/\text{W}$ , a large compression window is predicted, almost even encompassing Ti:Sapphire laser wavelengths. With the new large value,  $n_{\text{Kerr}}^I = 5.8 \cdot 10^{-20} \text{ m}^2/\text{W}$  the compression window starts opening around 900 nm, and taken the upper limit of the uncertainty,  $n_{\text{Kerr}}^I = 6.8 \cdot 10^{-20} \text{ m}^2/\text{W}$ , the compression window is only barely open at  $1.0 \mu\text{m}$ .

The experiments [5, 6] carried out at 800 nm were performed well into the nonstationary region, which was necessary to achieve a defocusing nonlinearity. No few-cycle compressed solitons were observed in [6], as the intensity had to be kept low in order to avoid severe GVM-induced self-steepening. (Note that the simulations in [6] actually used  $\chi^{(3)} = 5 \cdot 10^{-22} \text{ m}^2/\text{V}^2$ , corresponding to  $n_{\text{Kerr}}^I = 5.1 \cdot 10^{-20} \text{ m}^2/\text{W}$ , i.e. quite close to the values we find.) Instead the experiment carried out at 1250 nm [8] was done in the stationary regime, and indeed a few-cycle soliton was observed.

We should finally mention that the error made in assuming an isotropic response for the cascaded soliton compression is not large: most importantly, the crucial parameter is the FW SPM coefficient, which as we saw

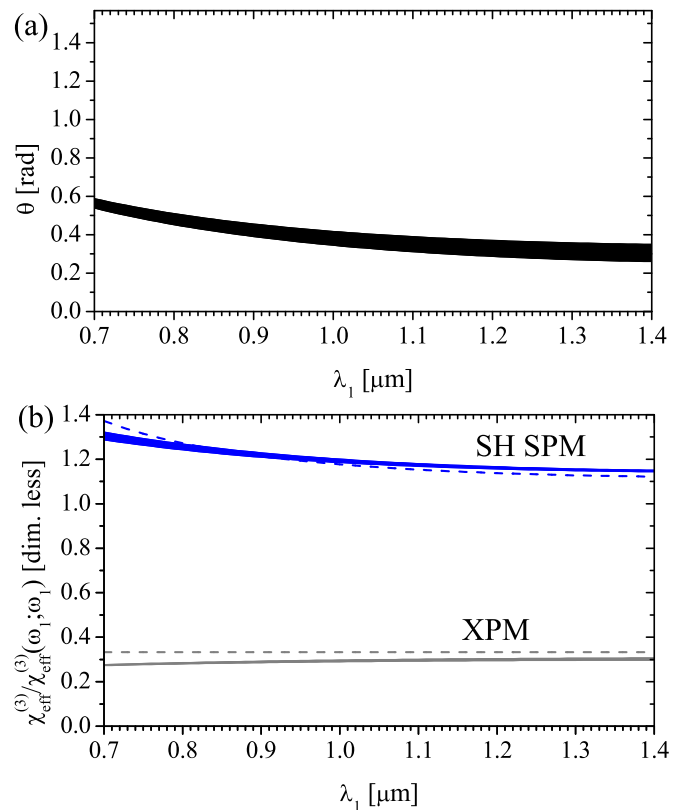


FIG. 3. Estimating the operating parameters vs. FW wavelength for cascaded SHG in BBO. (a) The  $\theta$ -range for which  $\Delta k > 0$  is achieved as well as  $|n_{\text{casc}}^I| > n_{\text{Kerr},11}^I$ . (b) The XPM term  $\chi_{\text{eff}}^{(3)}(\omega_1; \omega_2)$  and SH SPM term  $\chi_{\text{eff}}^{(3)}(\omega_2; \omega_2)$ , both normalized to the FW SPM term  $\chi_{\text{eff}}^{(3)}(\omega_1; \omega_1)$ . The range indicated corresponds to the  $\theta$  range in (a). The dashed lines indicate the isotropic limit. All nonlinear coefficients are scaled to other wavelengths using Miller's rule, and we used the SHG nonlinearities at 1064 nm from App. A as well as the cubic nonlinear parameters listed in Sec. III. For the SH SPM calculations the  $c_{33}$  parameter is unknown, but we used  $\chi_{33}^{(3)} = 1.0 \cdot 10^{-20} \text{ m}^2/\text{W}$  in the calculations. We also took  $\phi = \pi/6$  as this value optimizes the SHG nonlinearity.

is the same in the isotropic and in the anisotropic cases for this type I interaction. The XPM and SH SPM coefficients change when anisotropy is taken into account, but they play a minor role and rather tend to perturb the result more than shape it. In order to make a more quantitative statement, we calculated the  $\theta$ -ranges where self-defocusing solitons can be excited in BBO. A necessary (but not sufficient [19]) criterion for this to happen is  $\Delta k > 0$  as well as  $\Delta k$  low enough for  $|n_{\text{casc}}^I| > n_{\text{Kerr},11}^I$ . The range is shown vs. FW wavelength in Fig. 3(a). Inside this  $\theta$  range we can now for each wavelength calculate the anisotropic Kerr nonlinearities. As we know the FW SPM coefficient does not change with  $\theta$  (but it does change across the wavelength range shown, which we here estimate using Miller's rule), so we can normalize the results to this value. We then get the results shown

in Fig. 3(b). The XPM term is seen to lie close to the isotropic value  $1/3$  (found by taking  $\chi_{\text{eff}}^{(3)}(\omega_1; \omega_2) = c_{11}/3$ , dashed grey line), while the SH SPM term lies somewhat over 1. This is mainly caused by the wavelength scaling of the nonlinearity, which we confirmed by calculating the isotropic case (taking  $\chi_{\text{eff}}^{(3)}(\omega_2; \omega_2) = c_{11}$ , dashed blue line). In summary, assuming an isotropic response in BBO is a good approximation, mainly because the working  $\theta$  range lies close to zero (the isotropic limit). This result can therefore not be generalized to other nonlinear crystals, where the working range might lie closer to  $\pi/2$ .

### III. SUMMARY

In summary, our analysis of the experiments [11–17] points towards using the following Kerr nonlinearities

$$n_{\text{Kerr},11}^I = 5.8 \pm 1.0 \cdot 10^{-20} \text{ m}^2/\text{W}, \quad \lambda = 0.8 \text{ } \mu\text{m} \quad (34)$$

$$n_{\text{Kerr},10}^I = -0.25 \pm 0.04 \cdot 10^{-20} \text{ m}^2/\text{W}, \quad \lambda = 1.053 \text{ } \mu\text{m} \quad (35)$$

$$n_{\text{Kerr},16}^I = 1.5 \pm 0.4 \cdot 10^{-20} \text{ m}^2/\text{W}, \quad \lambda = 1.053 \text{ } \mu\text{m} \quad (36)$$

These values contain electronic as well as Raman contributions. We have indicated the wavelength, where the nonlinearities have been measured. In terms of the non-

linear susceptibility the values are

$$\chi_{11}^{(3)} = 5.6 \pm 0.9 \cdot 10^{-22} \text{ m}^2/\text{V}^2, \quad \lambda = 0.8 \text{ } \mu\text{m} \quad (37)$$

$$\chi_{10}^{(3)} = -0.24 \pm 0.04 \cdot 10^{-22} \text{ m}^2/\text{V}^2, \quad \lambda = 1.053 \text{ } \mu\text{m} \quad (38)$$

$$\chi_{16}^{(3)} = 1.4 \pm 0.4 \cdot 10^{-22} \text{ m}^2/\text{V}^2, \quad \lambda = 1.053 \text{ } \mu\text{m} \quad (39)$$

We have been unable to find experiments where the  $c_{33}$  component can be extracted.

The value  $n_{\text{Kerr},11}^I$  is considerably larger than the typical values used. Its value comes from a measurement in [11], but here we corrected the  $d_{\text{eff}}$  value used there to estimate the Kerr nonlinearity. We also corrected the Z-scan experiments [13, 14] for cascading contributions, that were to our knowledge erroneously neglected there.

### IV. ACKNOWLEDGMENTS

The Danish Council for Independent Research (grants no. 21-04-0506, 274-08-0479, and 11-106702) is acknowledged for support. Xianglong Zeng acknowledges the support of Marie Curie International Incoming Fellowship from EU (grant No. PIIIF-GA-2009–253289) and the financial support from National Natural Science Foundation of China (60978004) and Shanghai Shuguang Program (10SG38). Frank W. Wise, Jeffrey Moses and Satoshi Ashihara are acknowledged for useful discussions.

#### Appendix A: BBO crystal parameters

The crystal beta-barium-borate ( $\beta$ -BaB<sub>2</sub>O<sub>4</sub>, BBO) is a negative uniaxial crystal of the point group  $3m$ . The Sellmeier equations for were taken from Zhang et al. [32]. The quadratic nonlinear coefficients have been measured by Shoji et al. [29]: at  $\lambda = 1064 \text{ nm}$   $d_{22} = -2.2 \text{ pm/V}$ ,  $d_{31} = -d_{22}0.018 = 0.04 \text{ pm/V}$ , and  $d_{33} = 0.04 \text{ pm/V}$ , at  $\lambda = 852 \text{ nm}$   $d_{22} = -2.3 \text{ pm/V}$ , and at  $\lambda = 532 \text{ nm}$   $d_{22} = -2.6 \text{ pm/V}$ .

- 
- [1] L. A. Ostrovskii, “Self-action of light in crystals,” *Pisma Zh. Eksp. Teor. Fiz.* **5**, 331 (1967), [*JETP Lett.* **5**, 272–275 (1967)]
  - [2] J. M. R. Thomas and J. P. E. Taran, “Pulse distortions in mismatched second harmonic generation,” *Opt. Comm.* **4**, 329 – 334 (1972)
  - [3] C.C. Wang and E.L. Baardsen, “Optical third harmonic generation using mode-locked and non-mode-locked lasers,” *Appl. Phys. Lett.* **15**, 396397 (1969)
  - [4] R. DeSalvo, D.J. Hagan, M. Sheik-Bahae, G. Stegeman, E. W. Van Stryland, and H. Vanherzeele, “Self-focusing and self-defocusing by cascaded second-order effects in KTP,” *Opt. Lett.* **17**, 28–30 (1992)
  - [5] Xiang Liu, Liejia Qian, and Frank W. Wise, “High-energy pulse compression by use of negative phase shifts produced by the cascaded  $\chi^{(2)} : \chi^{(2)}$  nonlinearity,” *Opt. Lett.* **24**, 1777–1779 (1999)
  - [6] S. Ashihara, J. Nishina, T. Shimura, and K. Kuroda, “Soliton compression of femtosecond pulses in quadratic media,” *J. Opt. Soc. Am. B* **19**, 2505–2510 (2002)
  - [7] Jeffrey Moses and Frank W. Wise, “Soliton compression in quadratic media: high-energy few-cycle pulses with a frequency-doubling crystal,” *Opt. Lett.* **31**, 1881–1883 (2006)
  - [8] Jeffrey Moses and Frank W. Wise, “Controllable self-steepening of ultrashort pulses in quadratic nonlinear media,” *Phys. Rev. Lett.* **97**, 073903 (2006)
  - [9] Jeffrey Moses, Eihab Alhammali, Jason M. Eichenholz, and Frank W. Wise, “Efficient high-energy femtosecond pulse compression in quadratic media with flat-top beams,” *Opt. Lett.* **32**, 2469–2471 (2007)

- [10] M. Bache, O. Bang, B. B. Zhou, J. Moses, and F. W. Wise, "Optical Cherenkov radiation in ultrafast cascaded second-harmonic generation," *Phys. Rev. A* **82**, 063806 (2010)
- [11] Jeffrey Moses, Boris A. Malomed, and Frank W. Wise, "Self-steepening of ultrashort optical pulses without self-phase modulation," *Phys. Rev. A* **76**, 021802(R) (2007)
- [12] F. Hache, A. Zéboulon, G. Gallot, and G. M. Gale, "Cascaded second-order effects in the femtosecond regime in  $\beta$ -barium borate: self-compression in a visible femtosecond optical parametric oscillator," *Opt. Lett.* **20**, 1556–1558 (1995)
- [13] R. DeSalvo, A. A. Said, D.J. Hagan, E. W. Van Stryland, and M. Sheik-Bahae, "Infrared to ultraviolet measurements of two-photon absorption and  $n_2$  in wide bandgap solids," *IEEE J. Quantum Electron.* **32**, 1324–1333 (1996)
- [14] M. Sheik-Bahae and M. Ebrahimzadeh, "Measurements of nonlinear refraction in the second-order  $\chi^{(2)}$  materials  $\text{KTiOPO}_4$ ,  $\text{KNbO}_3$ ,  $\beta\text{-BaB}_2\text{O}_4$  and  $\text{LiB}_3\text{O}_5$ ," *Opt. Commun.* **142**, 294–298 (1997)
- [15] H. P. Li, C. H. Kam, Y. L. Lam, and W. Ji, "Femtosecond z-scan measurements of nonlinear refraction in nonlinear optical crystals," *Optical Materials* **15**, 237 – 242 (2001)
- [16] Paul S. Banks, Michael D. Feit, and Michael D. Perry, "High-intensity third-harmonic generation," *J. Opt. Soc. Am. B* **19**, 102–118 (2002)
- [17] R.A. Ganeev, I.A. Kulagin, A.I. Ryasnyansky, R.I. Tugushev, and T. Usmanov, "Characterization of nonlinear optical parameters of KDP,  $\text{LiNbO}_3$  and BBO crystals," *Opt. Commun.* **229**, 403–412 (2004)
- [18] M. Bache, O. Bang, J. Moses, and Frank W. Wise, "Nonlocal explanation of stationary and nonstationary regimes in cascaded soliton pulse compression," *Opt. Lett.* **32**, 2490–2492 (2007)
- [19] M. Bache, J. Moses, and F. W. Wise, "Scaling laws for soliton pulse compression by cascaded quadratic nonlinearities," *J. Opt. Soc. Am. B* **24**, 2752–2762 (2007)
- [20] M. Bache, O. Bang, W. Krolikowski, J. Moses, and Frank W. Wise, "Limits to compression with cascaded quadratic soliton compressors," *Opt. Express* **16**, 3273–3287 (2008)
- [21] M. Bache and F. W. Wise, "Type-I cascaded quadratic soliton compression in lithium niobate: Compressing femtosecond pulses from high-power fiber lasers," *Phys. Rev. A* **81**, 053815 (2010)
- [22] B. B. Zhou, A. Chong, F. W. Wise, and M. Bache, "Ultrafast and octave-spanning optical nonlinearities from strongly phase-mismatched quadratic interactions," *Phys. Rev. Lett.* **109**, 043902 (2012)
- [23] Carsten Langrock, M. M. Fejer, I. Hartl, and Martin E. Fermann, "Generation of octave-spanning spectra inside reverse-proton-exchanged periodically poled lithium niobate waveguides," *Opt. Lett.* **32**, 2478–2480 (2007)
- [24] C. R. Phillips, Carsten Langrock, J. S. Pelc, M. M. Fejer, I. Hartl, and Martin E. Fermann, "Supercontinuum generation in quasi-phasematched waveguides," *Opt. Express* **19**, 18754–18773 (2011)
- [25] Robert C. Miller, "Optical second harmonic generation in piezoelectric crystals," *Appl. Phys. Lett.* **5**, 17–19 (1964)
- [26] W. Ettoumi, Y. Petit, J. Kasparian, and J.-P. Wolf, "Generalized Miller formulæ," *Opt. Express* **18**, 6613–6620 (2010)
- [27] T. D. Krauss and F. W. Wise, "Femtosecond measurement of nonlinear absorption and refraction in CdS, ZnSe, and ZnS," *Appl. Phys. Lett.* **65**, 1739–1741 (1994)
- [28] Andrea Gnoli, Luca Razzari, and Marcofabio Righini, "Z-scan measurements using high repetition rate lasers: how to manage thermal effects," *Opt. Express* **13**, 7976–7981 (2005)
- [29] Ichiro Shoji, Hirotaka Nakamura, Keisuke Ohdaira, Takashi Kondo, Ryoichi Ito, Tsutomu Okamoto, Koichi Tatsuki, and Shigeo Kubota, "Absolute measurement of second-order nonlinear-optical coefficients of  $\beta\text{-BaB}_2\text{O}_4$  for visible to ultraviolet second-harmonic wavelengths," *J. Opt. Soc. Am. B* **16**, 620–624 (1999)
- [30] Jeffrey A. Moses(2010), private communication
- [31] M. Sheik-Bahae, D.C. Hutchings, D.J. Hagan, and E.W. Van Stryland, "Dispersion of bound electron nonlinear refraction in solids," *IEEE J. Quantum Electron.* **27**, 1296 –1309 (1991)
- [32] Dongxiang Zhang, Yufei Kong, and Jing-yuan Zhang, "Optical parametric properties of 532-nm-pumped beta-barium-borate near the infrared absorption edge," *Opt. Commun.* **184**, 485 – 491 (2000)